

# The Dynamic Nature of Coronary Artery Lesion Morphology Assessed by Serial Virtual Histology Intravascular Ultrasound Tissue Characterization

Takashi Kubo, MD, PhD,\* Akiko Maehara, MD,\* Gary S. Mintz, MD,\* Hiroshi Doi, MD, PhD,\* Kenichi Tsujita, MD, PhD,\* So-Yeon Choi, MD, PhD,\* Osamu Katoh, MD,† Kenya Nasu, MD,† Andreas Koenig, MD,‡ Michael Pieper, MD,§ Jason H. Rogers, MD,|| William Wijns, MD,¶ Dirk Böse, MD,# M. Paulina Margolis, MD, PhD,\*\* Jeffrey W. Moses, MD,\* Gregg W. Stone, MD,\* Martin B. Leon, MD\*

*New York, New York; Aichi, Japan; Munich and Essen, Germany; Kreuzlingen, Switzerland; Sacramento and San Diego, California; and Aalst, Belgium*

<b>Objectives</b>	We used virtual histology intravascular ultrasound (VH-IVUS) to investigate the natural history of coronary artery lesion morphology.
<b>Background</b>	Plaque stability is related to its histological composition.
<b>Methods</b>	We performed serial (baseline and 12-month follow-up) VH-IVUS studies and examined 216 nonculprit lesions (plaque burden $\geq 40\%$ ) in 99 patients. Lesions were classified into pathological intimal thickening (PIT), VH-IVUS-derived thin-capped fibroatheroma (VH-TCFA), thick-capped fibroatheroma (ThCFA), fibrotic plaque, and fibrocalcific plaque.
<b>Results</b>	At baseline, 20 lesions were VH-TCFAs; during follow-up, 15 (75%) VH-TCFAs “healed,” 13 became ThCFAs, 2 became fibrotic plaque, and 5 (25%) VH-TCFAs remained unchanged. Compared with VH-TCFAs that healed, VH-TCFAs that remained VH-TCFAs located more proximally (values are median [interquartile range]) (16 mm [15 to 18 mm] vs. 31 mm [22 to 47 mm], $p = 0.013$ ) and had larger lumen (9.1 mm <sup>2</sup> [8.2 to 10.7 mm <sup>2</sup> ] vs. 6.9 mm <sup>2</sup> [6.0 to 8.2 mm <sup>2</sup> ], $p = 0.021$ ), vessel (18.7 mm <sup>2</sup> [17.3 to 28.6 mm <sup>2</sup> ] vs. 15.5 mm <sup>2</sup> [13.3 to 16.6 mm <sup>2</sup> ]; $p = 0.010$ ), and plaque (9.7 mm <sup>2</sup> [9.6 to 15.7 mm <sup>2</sup> ] vs. 8.4 mm <sup>2</sup> [7 to 9.7 mm <sup>2</sup> ], $p = 0.027$ ) areas; however, baseline VH-IVUS plaque composition did not differ between VH-TCFAs that healed and VH-TCFAs that remained VH-TCFAs. Conversely, 12 new VH-TCFAs developed; 6 late-developing VH-TCFAs were PITs, and 6 were ThCFAs at baseline. In addition, plaque area at minimum lumen sites increased significantly in PITs (7.8 mm <sup>2</sup> [6.2 to 10.0 mm <sup>2</sup> ] to 9.0 mm <sup>2</sup> [6.5 to 12.0 mm <sup>2</sup> ], $p < 0.001$ ), VH-TCFAs (8.6 mm <sup>2</sup> [7.3 to 9.9 mm <sup>2</sup> ] to 9.5 mm <sup>2</sup> [7.8 to 10.8 mm <sup>2</sup> ], $p = 0.024$ ), and ThCFAs (8.6 mm <sup>2</sup> [6.8 to 10.2 mm <sup>2</sup> ] to 8.8 mm <sup>2</sup> [7.1 to 11.4 mm <sup>2</sup> ], $p < 0.001$ ) with a corresponding decrease lumen areas, but not in fibrous or fibrocalcific plaque.
<b>Conclusions</b>	Most VH-TCFAs healed during 12-month follow-up, whereas new VH-TCFAs also developed. PITs, VH-TCFAs, and ThCFAs showed significant plaque progression compared with fibrous and fibrocalcific plaque. (J Am Coll Cardiol 2010;55:1590–7) © 2010 by the American College of Cardiology Foundation

Autopsy data suggest that plaque composition is a key determinant of the propensity of atherosclerotic lesions to provoke clinical events (1). Fibroatheromas with a lipid-rich necrotic core (NC) and a thin fibrous cap (TCFA) seem particularly

prone to rupture and result in coronary artery occlusion (2–6). However, our knowledge about the genesis, progression, and

See page 1598

From the \*Cardiovascular Research Foundation, New York, New York; †Toyohashi Heart Center, Aichi, Japan; ‡Ludwig Maximilian University, Munich, Germany; §Herzzentrum Bodensee, Kreuzlingen, Switzerland; ||University of California, Davis Medical Center, Sacramento, California; ¶OLV Hospital, Aalst, Belgium; #University of Duisburg-Essen, Essen, Germany; and the \*\*Volcano Corporation, San Diego, California. Volcano Corporation (Rancho Cordova, California) has sponsored this registry. Dr. Kubo has received research grant support from Volcano Corporation.

Dr. Mintz is a member of the Speakers' Bureau, serves as a consultant, has received research/grant support, and is a stockholder with Volcano Corporation. Dr. Rogers is a consultant for Volcano Corporation. Dr. Margolis is an employee and stockholder with Volcano Corporation. Drs. Stone and Leon serve as consultants for Volcano Corporation.

Manuscript received April 8, 2009; revised manuscript received June 16, 2009, accepted July 14, 2009.

characterization of atherosclerosis is based mainly on cross-sectional histopathological studies. Intravascular ultrasound (IVUS) is the gold standard for evaluation of coronary plaques in vivo; however, conventional gray-scale IVUS has significant limitations in assessing atheromatous plaque composition and identifying TCFAs. Spectral analysis of IVUS radiofrequency backscattered signals, known as virtual histology IVUS (VH-IVUS), was developed to improve IVUS tissue characterization and provide detailed quantitative information on plaque composition in vivo (7). The aim of the present study was to use serial (baseline and follow-up) VH-IVUS to assess the natural history of coronary atherosclerotic plaques, in particular, the development and evolution of TCFAs.

## Methods

**Study population.** Between August 2004 and July 2006, 990 patients at 42 centers were enrolled in a prospective, multicenter, nonrandomized, global VH-IVUS registry. From this registry, we identified 99 patients with serial VH-IVUS examinations at baseline and follow-up for inclusion in the current analysis. Patients older than 18 years old without any contraindication to IVUS imaging undergoing diagnostic or interventional coronary procedures were enrolled in this study. Other than age younger 18 years, there were no enrollment exclusion criteria. Investigators were encouraged to repeat VH-IVUS imaging if the patient returned to the catheterization laboratory for any reason; repeat cardiac catheterization was performed routinely in 29 asymptomatic patients or because of symptom recurrence in 72 patients. The ethics committee at each participating institution approved the protocol, and written informed consent was obtained from all patients. Lipid disorder was defined as total cholesterol level  $\geq 200$  mg/dl, low-density lipoprotein cholesterol  $\geq 100$  mg/dl, high-density lipoprotein cholesterol  $< 50$  mg/dl, triglycerides  $\geq 150$  mg/dl, or medication use. Hypertension was defined as systolic blood pressure  $\geq 140$  mm Hg, diastolic blood pressure  $\geq 90$  mm Hg, or use of an antihypertensive drug. Patients with diabetes mellitus had a confirmed diagnosis or were using antidiabetic medications at study entry.

**IVUS image acquisition.** A phased-array, 20-MHz, 3.2-F IVUS catheter (Eagle Eye, Volcano Corporation, Rancho Cordova, California) was placed into the distal coronary artery and pulled back to the aorto-ostial junction using a motorized catheter pull-back system set at 0.5 mm/s. During pullback, gray-scale IVUS was recorded, raw radiofrequency data were captured at the top of the R wave, and reconstruction of the color-coded map by a VH-IVUS data recorder was performed (In-Vision Gold, Volcano Corporation). The gray-scale IVUS and captured radiofrequency data were written onto a CD-R or DVD-R, respectively.

**Gray-scale and VH-IVUS analyses.** Off-line gray-scale and VH-IVUS analyses were performed by pcVH 2.1 software (Volcano Corporation). Corresponding images of baseline and follow-up IVUS examinations were identified

by the distance from 2 fiducial landmarks such as side branches and stent edges. Gray-scale IVUS measurements of lumen, external elastic membrane (EEM), and plaque and media (P&M, defined as EEM minus lumen) cross-sectional areas and plaque burden (defined as P&M divided by EEM) were performed for every recorded frame (8). We identified nonculprit, untreated lesions as having a plaque burden  $\geq 40\%$  in at least 3 consecutive frames ( $\sim 1.5$  mm in length). VH-IVUS analysis of these nonculprit, untreated lesions was also performed for every recorded frame. The 4 VH-IVUS plaque components were color-coded as white (dense calcium [DC]), red (NC), light green (fibrofatty [FF]), and dark green (fibrotic tissue [FT]) and reported as percentages of plaque area and total plaque volume (7).

Volumetric gray-scale and VH-IVUS analyses were performed using Simpson's rule.

**Definition of lesion types.** Lesions were classified by 2 experienced, independent observers (T.K. and A.M.) based on plaque composition: pathological intimal thickening (PIT), virtual histology intravascular ultrasound-derived TCFA (VH-TCFA), thick-capped fibroatheroma (ThCFA), fibrotic plaque, and fibrocalcific plaque (9,10) (Fig. 1). PIT consisted of mainly a mixture of FT and FF plaque with  $< 10\%$  confluent NC and  $< 10\%$  confluent DC. VH-TCFA was a fibroatheroma without evidence of a fibrous cap:  $> 10\%$  confluent NC with  $> 30^\circ$  NC abutting the lumen in at least 3 consecutive frames. ThCFA was a fibroatheroma ( $> 10\%$  of confluent NC in at least 3 consecutive frames) with a definable fibrous cap. Fibroatheromas with features of both VH-TCFAs and ThCFAs were classified as VH-TCFAs. Fibrotic plaque consisted of mainly fibrous tissue with  $< 10\%$  confluent NC,  $< 15\%$  FF tissue, and  $< 10\%$  confluent DC. Fibrocalcific plaque was composed of nearly all FT and DC with  $< 10\%$  confluent NC.

**Statistical analysis.** Categorical variables were presented as frequencies, with comparison using chi-square statistics or the Fisher exact test (if there was an expected cell value  $< 5$ ). Continuous variables were presented as medians and interquartile ranges and were compared using Mann-Whitney U test or the Wilcoxon signed rank test. The changes in lumen and P&M area during follow-up were compared among 5 plaque types by Kruskal-Wallis analysis using Steel-Dwass test for multiple comparisons. A p value  $< 0.05$  was considered statistically significant. Intraobserver variability and

## Abbreviations and Acronyms

<b>DC</b>	= dense calcium
<b>EEM</b>	= external elastic membrane
<b>FF</b>	= fibrofatty
<b>FT</b>	= fibrotic tissue
<b>IVUS</b>	= intravascular ultrasound
<b>NC</b>	= necrotic core
<b>PIT</b>	= pathological intimal thickening
<b>P&amp;M</b>	= plaque and media
<b>TCFA</b>	= thin-capped fibroatheroma
<b>ThCFA</b>	= thick-capped fibroatheroma
<b>VH-IVUS</b>	= virtual histology intravascular ultrasound
<b>VH-TCFA</b>	= virtual histology intravascular ultrasound-derived thin-capped fibroatheroma

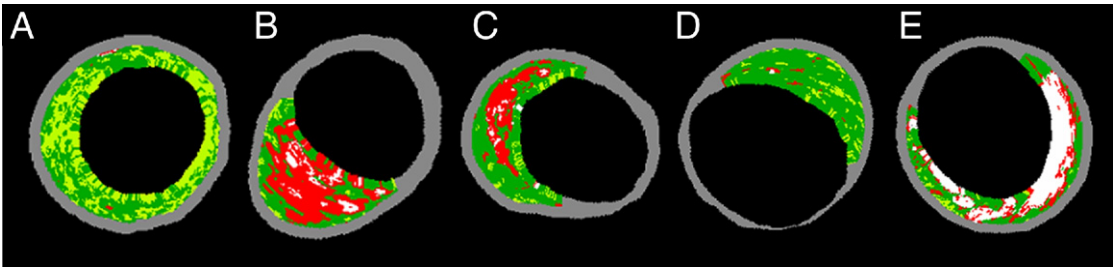


**Figure 1** Plaque Classification by VH-IVUS

(A) Pathological intimal thickening. (B) Virtual histology intravascular ultrasound (VH-IVUS)-derived thin-capped fibroatheroma. (C) Thick-capped fibroatheroma. (D) Fibrotic plaque. (E) Fibrocalcific plaque.

interobserver variability for lesion type classifications were measured by  $\kappa$  test of concordance using the data without correction for correlated observations within individuals.

Results

**Patient and lesion characteristics.** Baseline patient characteristics are listed in Table 1. The follow-up period was 12 (interquartile range [IQR] 7 to 14) months. Systolic blood pressure (136 mm Hg [IQR 120 to 160 mm Hg] to 135 mm Hg [IQR 120 to 148 mm Hg],  $p = 0.005$ ) and diastolic blood pressure (80 mm Hg [IQR 72 to 82 mm Hg] to 78 mm Hg [IQR 68 to 80 mm Hg],  $p = 0.011$ ) decreased significantly during follow-up. There were no significant differences in the serum levels of total cholesterol (193

mg/dl [162 to 221 mg/dl] to 187 mg/dl [IQR 164 to 213 mg/dl],  $p = 0.2$ ), low-density lipoprotein cholesterol (111 mg/dl [IQR 88 to 132 mg/dl] to 103 mg/dl [IQR 85 to 127 mg/dl],  $p = 0.1$ ), and high-density lipoprotein cholesterol (47 mg/dl [IQR 37 to 58 mg/dl] to 49 mg/dl [IQR 40 to 57 mg/dl],  $p = 0.1$ ) between baseline and follow-up. Overall, 216 nonculprit, untreated lesions were identified, analyzed by gray-scale and VH-IVUS, and classified as PIT ( $n = 62$ ), VH-TCFA ( $n = 20$ ), ThCFA ( $n = 93$ ), fibrous plaque ( $n = 22$ ), and fibrocalcific plaque ( $n = 19$ ), as shown in Table 2. Intraobserver and interobserver variability yielded good concordance for lesion type classifications ( $\kappa = 0.90$  and  $\kappa = 0.87$ , respectively).

**Serial gray-scale IVUS analysis.** The P&M area at the minimum lumen site increased significantly during follow-up in PITs (7.8 mm<sup>2</sup> [IQR 6.2 to 10.0 mm<sup>2</sup>] to 9.0 mm<sup>2</sup> [IQR 6.5 to 12.0 mm<sup>2</sup>],  $p < 0.001$ ), VH-TCFAs (8.6 mm<sup>2</sup> [IQR 7.3 to 9.9 mm<sup>2</sup>] to 9.5 mm<sup>2</sup> [IQR 7.8 to 10.8 mm<sup>2</sup>],  $p = 0.024$ ), and ThCFAs (8.6 mm<sup>2</sup> [IQR 6.8 to 10.2 mm<sup>2</sup>] to 8.8 mm<sup>2</sup> [IQR 7.1 to 11.4 mm<sup>2</sup>],  $p < 0.001$ ), but not in fibrotic or fibrocalcific plaque. The increase in P&M area was significantly greater in PITs, VH-TCFAs, and ThCFAs compared with fibrocalcific plaque (Fig. 2). Correspondingly, the minimum lumen area decreased significantly in PITs (8.2 mm<sup>2</sup> [IQR 6.3 to 10.5 mm<sup>2</sup>] to 7.2 mm<sup>2</sup> [IQR 5.2 to 9.6 mm<sup>2</sup>],  $p < 0.001$ ), VH-TCFAs (7.2 mm<sup>2</sup> [IQR 6.2 to 9.0 mm<sup>2</sup>] to 6.8 mm<sup>2</sup> [IQR 5.6 to 8.3 mm<sup>2</sup>],  $p = 0.005$ ), and ThCFAs (6.8 mm<sup>2</sup> [IQR 5.3 to 8.4 mm<sup>2</sup>] to 6.4 mm<sup>2</sup> [IQR 4.4 to 8.5 mm<sup>2</sup>],  $p < 0.001$ ), but not in fibrotic or fibrocalcific plaque. The decrease in minimum lumen area was significantly greater in PITs compared with ThCFAs, fibrotic plaque, and fibrocalcific plaque (Fig. 2).

**Serial VH-IVUS analysis.** During follow-up, the percentage of NC area at the minimum lumen site increased significantly in PITs (8% [IQR 4% to 12%] to 11% [IQR 5% to 21%],  $p = 0.008$ ), but decreased significantly in VH-TCFAs (32% [IQR 23% to 36%] to 21% [IQR 15% to 24%],  $p < 0.001$ ) and ThCFAs (22% [IQR 17% to 28%] to 20% [IQR 15% to 26%],  $p = 0.043$ ). The percentage of NC area in fibrotic plaque and fibrocalcific plaque did not

**Table 1** Clinical Patient Characteristics at Baseline and Follow-up

	Baseline	Follow-up
Age, yrs	66 (55–73)	67 (56–74)
Male sex	78	78
Clinical presentation		
ACS/none-ACS	23/77	0/100
Target coronary vessel		
LAD/LCX/RCA	54/20/26	54/20/26
Previous MI	43	46
Coronary risk factors		
Hypertension	72	72
Diabetes	31	31
Lipid disorder	71	74
Smoker	55	58
Family history of CAD	43	43
Medications		
Antiplatelet agent	85	96
Beta-blocker	51	49
ACEI/ARB	30	42
Calcium-channel blocker	31	30
Insulin	7	7
Statin	53	69

Values are given as median and interquartile range or %.  
ACEI = angiotensin-converting enzyme inhibitor; ACS = acute coronary syndrome; ARB = angiotensin receptor blocker; CAD = coronary artery disease; LAD = left anterior descending; LCX = left circumflex; RCA = right coronary artery.

Table 2 Changes of Intravascular Ultrasound Findings Between Baseline and Follow-Up

	PIT (n = 62)		VH-TCFA (n = 20)		ThCFA (n = 93)		Fibrotic (n = 22)		Fibrocalcific (n = 19)	
	Baseline	Follow-Up	Baseline	Follow-Up	Baseline	Follow-Up	Baseline	Follow-Up	Baseline	Follow-Up
Minimum lumen site										
Lumen area, mm <sup>2</sup>	8.2 (6.3-10.5)	7.2 (5.2-9.6)*	7.2 (6.2-9.0)	6.8 (5.6-8.3)*	6.8 (5.3-8.4)	6.4 (4.4-8.5)*	7.5 (5.7-10.7)	7.4 (6.1-10.7)	8.1 (7.3-9.7)	8.1 (6.8-19.7)
EEM area, mm <sup>2</sup>	15.5 (13.0-19.5)	16.1 (13.4-20.2)	16.0 (14.7-18.1)	15.4 (13.8-17.9)	15.6 (12.8-17.9)	15.5 (12.6-18.7)	17.5 (12.2-19.2)	17.3 (11.8-19.5)	16.9 (15.8-18.8)	17.1 (15.1-19.4)
P&M area, mm <sup>2</sup>	7.8 (6.2-10.0)	9.0 (6.5-12.0)*	8.6 (7.3-9.9)	9.5 (7.8-10.8)*	8.6 (6.8-10.2)	8.8 (7.1-11.4)*	7.9 (6.0-10.7)	8.0 (6.5-11.3)	9.2 (6.8-10.8)	9.3 (7.2-11.0)
Plaque burden, %	47 (41-56)	55 (49-62)*	54 (51-58)	58 (53-63)*	55 (49-62)	56 (49-67)*	49 (44-56)	51 (47-58)	53 (44-58)	53 (44-62)
DC, %	1 (1-2)	2 (1-4)*	11 (7-14)	8 (5-15)	11 (7-19)	12 (7-16)	2 (1-4)	2 (1-5)	24 (21-32)	27 (17-35)
NC, %	8 (4-12)	11 (5-21)*	32 (23-36)	21 (15-24)*	22 (17-28)	20 (15-26)*	9 (6-11)	8 (6-17)	22 (18-30)	24 (20-29)
FF, %	21 (14-30)	20 (12-26)	8 (4-12)	13 (11-21)*	10 (6-17)	12 (7-20)	11 (8-13)	17 (9-22)*	7 (5-11)	8 (3-11)
FT, %	67 (62-74)	65 (58-69)	49 (44-55)	51 (47-59)	53 (44-60)	53 (47-60)	78 (72-79)	68 (61-72)*	42 (34-52)	45 (34-51)
Volumetric analysis										
P&M volume, mm <sup>3</sup>	44.4 (28.9-81.3)	50.8 (31.5-94.1)*	77.4 (48.0-104.2)	82.0 (57.7-117.4)*	70.3 (35.1-113.2)	74.4 (35.7-107.3)	42.5 (20.0-65.8)	44.1 (20.4-68.0)	77.4 (39.8-118.9)	81.2 (39.9-121.2)
DC, %	2 (1-4)	4 (1-6)*	9 (7-12)	7 (4-13)	10 (6-17)	11 (7-15)	3 (2-4)	5 (1-7)	17 (9-24)	14 (10-20)
NC, %	8 (5-13)	10 (6-16)	25 (20-29)	17 (12-20)*	20 (14-25)	19 (12-22)	9 (6-12)	9 (6-16)	16 (11-26)	19 (16-22)
FF, %	21 (17-31)	22 (15-28)	10 (8-13)	17 (12-20)*	12 (9-18)	14 (10-20)	12 (10-14)	18 (12-26)*	11 (4-19)	13 (8-17)
FT, %	65 (59-69)	63 (58-67)	55 (49-58)	56 (50-60)	56 (49-60)	55 (49-60)	75 (72-79)	63 (58-70)*	55 (43-60)	55 (47-57)

Values are given as median (interquartile range). \*p < 0.05 vs. baseline. DC = dense calcium; EEM = external elastic membrane; FF = fibrofatty; FT = fibrotic tissue; NC = necrotic core; P&M = plaque and media; PIT = pathological intimal thickening; TCFA = thin-capped fibroatheroma; ThCFA = thick-capped fibroatheroma.

change between baseline and follow-up. Volumetric VH-IVUS analysis supported these observations. Data are shown in Table 2.

**Evolution of nonculprit coronary lesions.** At baseline, there were 20 VH-TCFAs. During follow-up, 15 (75%) VH-TCFAs healed by evolving into a different lesion type, 13 became ThCFAs, and 2 became fibrotic plaques, whereas 5 (25%) VH-TCFAs remained unchanged (Fig. 3). Compared with VH-TCFAs that healed, VH-TCFAs that remained unchanged located more proximally (distance from coronary ostium to the lesion of 16 mm [IQR 15 to 18 mm] vs. 31 mm [IQR 22 to 47 mm], respectively, p = 0.013) and had larger lumen areas (9.1 mm<sup>2</sup> [IQR 8.2 to 10.7 mm<sup>2</sup>] vs. 6.9 mm<sup>2</sup> [IQR 6.0 to 8.2 mm<sup>2</sup>], p = 0.021), EEM areas (18.7 mm<sup>2</sup> [IQR 17.3 to 28.6 mm<sup>2</sup>] vs. 15.5 mm<sup>2</sup> [IQR 13.3 to 16.6 mm<sup>2</sup>], p = 0.010), and P&M areas (9.7 mm<sup>2</sup> [IQR 9.6 to 15.7 mm<sup>2</sup>] vs. 8.4 mm<sup>2</sup> [IQR 7.2 to 9.7 mm<sup>2</sup>], p = 0.027); however, baseline VH-IVUS plaque composition was not different between VH-TCFAs that healed versus VH-TCFAs that remained unchanged. Healing of VH-TCFAs was not related to acute coronary presentations at baseline (p = 0.3), follow-up duration (p = 0.7), angiotensin-converting enzyme inhibitor/angiotensin receptor blocker administration (p = 0.2), statin administration (p = 0.2), or change in serum low-density lipoprotein levels during follow-up (p = 0.9).

During follow-up, 12 new VH-TCFAs developed; 6 new VH-TCFAs were PIT and 6 were ThCFAs at baseline. There was no difference in baseline characteristics between PITs that evolved into VH-TCFAs compared with PITs that did not develop into VH-TCFAs. Although the percentage of NC area at baseline was not different between ThCFAs that evolved into VH-TCFAs compared with ThCFAs that did not develop into VH-TCFAs, the percentage of DC area (4% [IQR 2% to 5%] vs. 11% [IQR 8% to 20%], p = 0.006) was significantly lower in ThCFAs that evolved into VH-TCFAs. During the follow-up period, no lesions resulted in acute coronary events, including the 12 “new” VH-TCFAs. Representative serial IVUS images at baseline and follow-up are shown in Figure 4.

Discussion

This is the first report to use serial VH-IVUS to assess the natural history of coronary artery lesion morphology in vivo. The major findings of our analysis are as follows. 1) Most VH-TCFAs stabilized or healed during 12 months of follow-up. Only proximal VH-TCFAs in larger vessels with more plaque appeared to heal less often. 2) New VH-TCFAs developed from PITs or ThCFAs. 3) Lesions classified as PIT, VH-TCFA, and ThCFA showed significant progression (increase plaque and decrease in lumen) compared with fibrotic and fibrocalcific plaque.

**Histological classification of atherosclerotic plaque.** Based on histological composition and structure, the American Heart Association’s Committee on Vascular Lesions



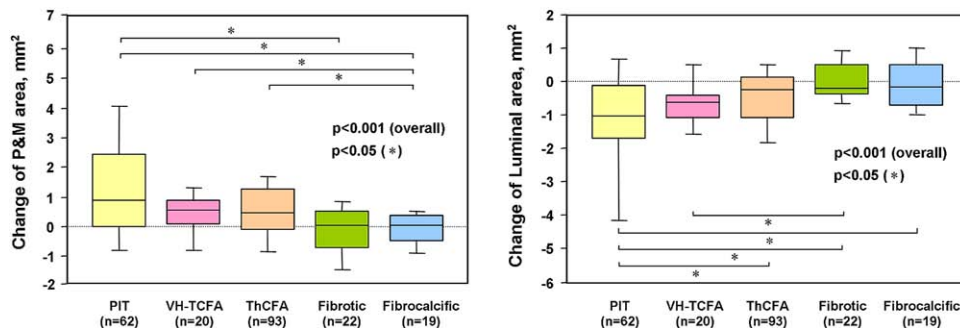


**Figure 2** Changes in P&M Area and Lumen Area During Follow-Up

The increase of plaque and media (P&M) area and the decrease in minimum lumen were significantly different among lesion phenotypes and were greater in lesions classified as pathologic intimal thickening (PIT) compared with fibrotic or fibrocalcific lesions. ThCFA = thick-capped fibroatheroma; VH-TCFA = virtual histology–derived thin-capped fibroatheroma.

recommended a practical classification of human atherosclerotic lesions that provided a basis for understanding changes in progression, stabilization, or regression of atherosclerotic

lesions (1). Virmani et al. (4) proposed TCFA as a specific lesion type that was a precursor of plaque rupture. Subsequent studies defined TCFA fibrous cap thickness as  $<65 \mu\text{m}$  (2) and showed that nearly 75% of TCFA had  $>10\%$  of the plaque area occupied by a lipid-rich NC (3). Atherosclerotic lesions were subsequently classified into intimal xanthoma, intimal thickening, PIT, fibrous cap atheroma, TCFA, calcified nodule, and fibrocalcific plaque (4). Based on post-mortem histology data, this specific lesion classification allowed correlation with morphology determined by clinically applicable diagnostic measurements including newer in vivo imaging techniques such as VH-IVUS.

Tissue characterization by VH-IVUS is a potential tool to enable an accurate evaluation of the coronary plaque composition. Nair et al. (7), in a histological study, reported that VH-IVUS had an 80% to 92% accuracy for identification of coronary plaque DC, NC, FF, or FT. Subsequent studies demonstrated the high reproducibility of VH-IVUS analyses (11,12). Hartmann et al. (12) showed that the relative difference of volumetric VH-IVUS analysis in repeated pull-backs was  $<1\%$  for NC and  $<3\%$  for DC, FF, and FT. These studies formed the backbone of the current serial VH-IVUS analysis. In the present VH-IVUS study, coronary lesions were classified as PIT, VH-TCFA, ThCFA, fibrotic plaque, and fibrocalcific plaques, similar to the histopathological classification. Presumably, this VH-IVUS classification also represented the different stages of development of atherosclerosis from early intimal thickening to vulnerable lesions (such as VH-TCFA) to stable fibrocalcific disease.

**VH-TCFAs.** Using VH-IVUS in a small number of patients, Rodriguez-Granillo et al. (9) reported that VH-TCFAs were detected 3 times as often in secondary, nonobstructive lesions of acute coronary syndrome patients compared with stable angina patients. In a larger VH-IVUS analysis, Hong et al. (13) reported that primary lesions of acute coronary syndrome patients more often contained

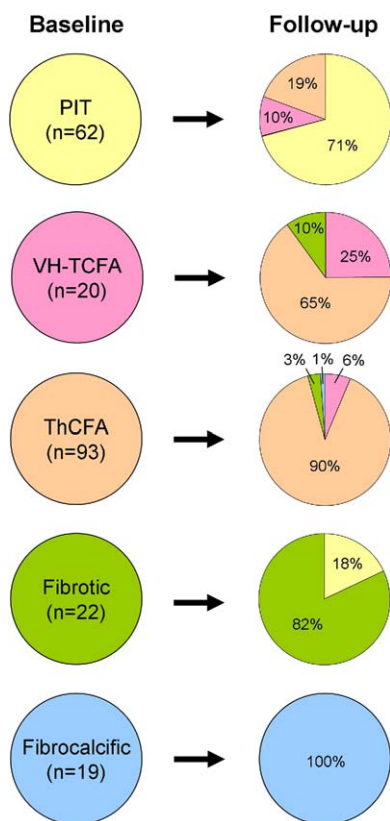


**Figure 3** Changes in Plaque Characteristics Assessed by VH-IVUS Between Baseline and Follow-Up

During follow-up, 75% of VH-TCFAs evolved into ThCFA or fibrotic plaque and 25% remain unchanged. Conversely, 10% of PITs and 6% of ThCFAs evolved into VH-TCFAs. No fibrotic plaque and fibrocalcific plaque evolved into fibroatheromas. Abbreviations as in Figures 1 and 2.

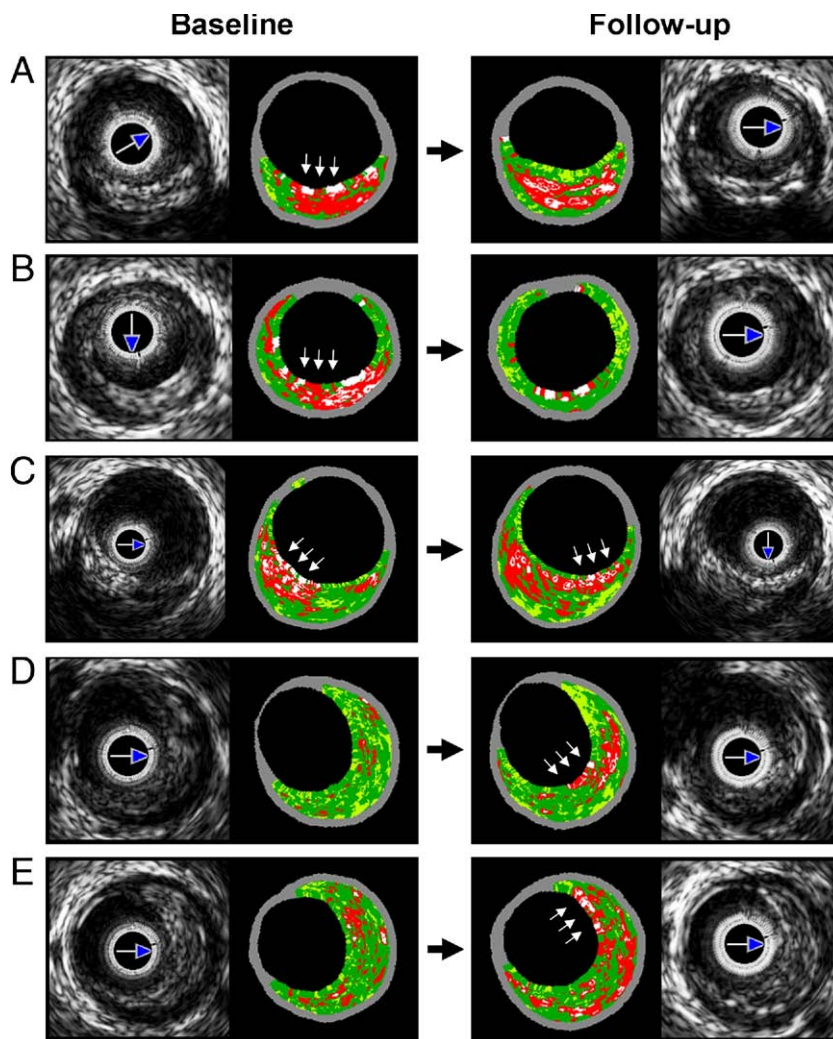


**Figure 4** Representative Images of Serial Intravascular Ultrasound at Baseline and Follow-Up

(A) VH-TCFAs became ThCFAs. (B) VH-TCFAs became fibrous plaques. (C) VH-TCFAs remained unchanged, although the location of the necrotic core in contact with the lumen shifted axially (arrows). (D) PITs became VH-TCFAs. (E) ThCFAs became VH-TCFAs. Abbreviations as in Figures 1 and 2.

VH-TCFAs (as well as already ruptured plaques) than those of stable angina patients (89% vs. 62%,  $p < 0.001$ ). Furthermore, in a 3-vessel VH-IVUS analysis, they demonstrated that the overall frequency of VH-TCFAs was 2.5 per patient with acute coronary syndrome versus 1.7 per patient with stable angina ( $p < 0.001$ ) (14). However, none of these studies examined that natural history of this lesion subset.

**Natural history of TCFAs.** There are various possible pathways in the evolution and stabilization of TCFAs. According to pathologic studies, TCFAs are precursor lesions for plaque rupture. The thin, fibrous cap is distinguished by the loss of smooth muscle cells, extracellular matrix, and inflammatory infiltrate. In a series of >200 sudden death cases, approximately 60% of acute thrombi resulted from rupture of a TCFA (4). Other relevant

features that contribute to plaque rupture include the extent of inflammation in the fibrous cap, fissuring, calcification, intraplaque vasa vasorum, and intraplaque hemorrhage.

However, not all TCFAs rupture, although the mechanism of healing of TCFAs is not well established. The transformation of hematoma and/or thrombus into fibromuscular tissue and the formation or increase in thickness of the fibrous cap could lead to plaque stabilization (1). Virmani *et al.* (3) and Burke *et al.* (5) proposed that a silent plaque rupture or a plaque rupture proximal to a lesion might lead to mural thrombus and subsequent formation of a fibrotic cap over the TCFA. Moreover, many animal and clinical studies have shown that changes in the plaque environment, such as a reduction in plasma lipid concentrations, can stabilize and cause regression of even advanced lesions (15). The American Heart Association recommen-

dation suggests that fibroatheromas may become fibrocalcific lesions without developing complex features such as surface defects, hematoma/hemorrhage, and/or thrombosis (1). In the present VH-IVUS study, most (75%) VH-TCFAs healed or stabilized to become ThCFAs or fibrotic plaques, and new VH-TCFAs developed from PITs and ThCFAs during 12 months of follow-up. Furthermore, no lesions resulted in plaque rupture or caused acute events, including “new” VH-TCFAs. Previous IVUS studies showed that plaque rupture itself does not necessarily cause acute events unless there is thrombus formation with significant lumen compromise (16). However, the current population of VH-TCFAs had little lumen compromise, and this might have contributed to a lack of clinical events.

Coronary artery TCFAs occur in a limited, focal distribution as do plaque ruptures and acute occlusions. Cheruvu et al. (6) longitudinally sectioned coronary arteries to show that TCFAs clustered in the proximal coronary arteries; 50% of TCFAs were present within the first 22 mm and 90% within the first 33 mm of the left anterior descending and left circumflex arteries, and 50% of TCFAs were observed within the first 31 mm and 90% within the first 74 mm of the right coronary artery. In an angiographic study, Wang et al. (17) showed that acute coronary occlusions leading to ST-segment elevation myocardial infarction tended to cluster in predictable “hot spots” within the proximal third of the coronary arteries. Hong et al. (18) performed 3-vessel gray-scale IVUS to demonstrate that plaque ruptures occur mainly in proximal segments (83%) of the left anterior descending artery, the proximal (48%) and distal (32%) segments of the right coronary artery, and the entire left circumflex artery. Using VH-IVUS, Valgimigli et al. (19) confirmed that plaque composition had a nonuniform distribution, with proximal segments having a significantly larger NC compared with distal segments (mean 13% vs. 8.7%,  $p < 0.05$ ). Moreover, VH-TCFAs were more common in proximal coronary artery segments compared with distal segments (9). The present study extends these observations to show that proximal VH-TCFAs in larger vessels with more plaque seemed to heal less often compared with distal VH-TCFAs and that this might contribute to plaque rupture and subsequent thrombosis.

**VH-IVUS assessment of the natural history of coronary artery disease.** Identification of coronary lesions at significant risk of plaque progression is of great clinical importance. Post-mortem studies have clearly shown that subclinical and repeated plaque rupture followed by healing have a key role in plaque progression (5). Younger patient age, unstable clinical presentation, and overall severity of angiographic coronary artery disease have been proposed as predictors of rapid coronary stenosis progression (20). In a serial angiographic study, Kaski et al. (21) showed that mean stenosis diameter reduction was significantly greater in complex lesions than in smooth lesions (11.6% vs. 3.9% change;  $p < 0.001$ ). In a serial gray-scale IVUS study, Berry et al. (22) demonstrated that patients with angiographic

progression had greater plaque volume at baseline on IVUS ( $p = 0.0495$ ) and a significantly greater increase in plaque volume from baseline to follow-up ( $p = 0.0283$ ) compared with patients with no angiographic progression. The present study extends these previous observations by demonstrating varying degrees of plaque progression among the 5 VH-IVUS lesion subtypes. Lesions classified as PIT, VH-TCFA, and ThCFA showed significant progression (increase in plaque mass and decrease in lumen area) compared with fibrotic and fibrocalcific plaque in which there were no geometric changes during 12 months of follow-up.

The IBIS-1 (Integrated Biomarker and Imaging Study-1) substudy assessed the correlation between temporal changes in plaque composition and circulating biomarkers (23). Subsequently, the IBIS-2 study demonstrated that lipoprotein-associated phospholipase A<sub>2</sub> inhibition prevented NC growth within coronary atherosclerotic plaques (24). The PROSPECT (Providing Regional Observation to Study Predictors of Events in the Coronary Tree) trial was designed to use VH-IVUS to detect high-risk, rupture-prone lesions. The SPECIAL (Study of Prospective Events in Coronary Intermediate Atherosclerotic Lesions) was designed to correlate lesion characteristics, patient risk factors, and other measurements with subsequent cardiac events as well as plaque progression and regression. VH-IVUS may provide critical new information about the role of vulnerable plaque and about the natural progression of coronary artery disease.

**Study limitations.** First, this was a registry study and not representative of the whole spectrum of patients with coronary heart disease with follow-up at the discretion of the investigators. Larger serial VH-IVUS studies with longer term follow-up may help to distinguish plaques prone to rupture and, as a consequence, to lead to cardiac events. Second, the present study evaluated only nonculprit lesions with modest plaque burden that were not accompanied by significant lumen narrowing. Third, the axial resolution of VH-IVUS (100 to 200  $\mu\text{m}$ ) was inadequate to detect critical fibrous cap thickness, currently defined as  $<65 \mu\text{m}$ . Finally, the limited longitudinal resolution of VH-IVUS imaging, based on electrocardiography-triggered cross-sectional analysis, may have biased the identification of corresponding images in serial (baseline and follow-up) VH-IVUS studies.

## Conclusions

Plaque stability is related to its histological composition. Although most VH-TCFAs seem to stabilize or heal during follow-up, proximal VH-TCFAs in larger vessels with more plaque appear to heal less often. Moreover, new VH-TCFAs can develop from PIT or ThCFA. Lesions classified as PIT, VH-TCFA, and ThCFA showed significant



plaque progression compared with fibrous and fibrocalcific plaque. In comparison with other clinically available, catheter-based, intracoronary diagnostic tools, VH-IVUS may be useful in assessing the natural history of stable and unstable atherosclerotic lesions.

**Reprint requests and correspondence:** Dr. Akiko Maehara, Cardiovascular Research Foundation, 111 East 59th Street, New York, New York 10022. E-mail: [amaehara@crf.org](mailto:amaehara@crf.org).

## REFERENCES

1. Stary HC. Natural history and histological classification of atherosclerotic lesions: an update. *Arterioscler Thromb Vasc Biol* 2000;20:1177–8.
2. Burke AP, Farb A, Malcom GT, et al. Coronary risk factors and plaque morphology in men with coronary disease who died suddenly. *N Engl J Med* 1997;336:1276–82.
3. Virmani R, Burke AP, Farb A, et al. Pathology of the vulnerable plaque. *J Am Coll Cardiol* 2006;47:C13–8.
4. Virmani R, Kolodgie FD, Burke AP, et al. Lessons from sudden coronary death: a comprehensive morphological classification scheme for atherosclerotic lesions. *Arterioscler Thromb Vasc Biol* 2000;20:1262–75.
5. Burke AP, Kolodgie FD, Farb A, et al. Healed plaque ruptures and sudden coronary death: evidence that subclinical rupture has a role in plaque progression. *Circulation* 2001;103:934–40.
6. Cheruvu PK, Finn AV, Gardner C, et al. Frequency and distribution of thin-cap fibroatheroma and ruptured plaques in human coronary arteries: a pathologic study. *J Am Coll Cardiol* 2007;50:940–9.
7. Nair A, Kuban BD, Tuzcu EM, Schoenhagen P, Nissen SE, Vince DG. Coronary plaque classification with intravascular ultrasound radiofrequency data analysis. *Circulation* 2002;106:2200–6.
8. Mintz GS, Nissen SE, Anderson WD, et al. American College of Cardiology clinical expert consensus document on standards for acquisition, measurement and reporting of intravascular ultrasound studies (IVUS). A report of the American College of Cardiology Task Force on Clinical Expert Consensus Documents. *J Am Coll Cardiol* 2001;37:1478–92.
9. Rodriguez-Granillo GA, García-García HM, McFadden EP, et al. In vivo intravascular ultrasound-derived thin-cap fibroatheroma detection using ultrasound radiofrequency data analysis. *J Am Coll Cardiol* 2005;46:2038–42.
10. König A, Margolis MP, Virmani R, et al. Technology insight: in vivo coronary plaque classification by intravascular ultrasonography radiofrequency analysis. *Nat Clin Pract Cardiovasc Med* 2008;5:219–29.
11. Rodriguez-Granillo GA, Vaina S, García-García HM, et al. Reproducibility of intravascular ultrasound radiofrequency data analysis: implications for the design of longitudinal studies. *Int J Cardiovasc Imaging* 2006;22:621–31.
12. Hartmann M, Mattern ES, Huisman J, et al. Reproducibility of volumetric intravascular ultrasound radiofrequency-based analysis of coronary plaque composition in vivo. *Int J Cardiovasc Imaging* 2009;25:13–23.
13. Hong MK, Mintz GS, Lee CW, et al. Comparison of virtual histology to intravascular ultrasound of culprit coronary lesions in acute coronary syndrome and target coronary lesions in stable angina pectoris. *Am J Cardiol* 2007;100:953–9.
14. Hong MK, Mintz GS, Lee CW, et al. A three-vessel virtual histology intravascular ultrasound analysis of frequency and distribution of thin-cap fibroatheromas in patients with acute coronary syndrome or stable angina pectoris. *Am J Cardiol* 2008;101:568–72.
15. Williams KJ, Feig JE, Fisher EA. Rapid regression of atherosclerosis: insights from the clinical and experimental literature. *Nat Clin Pract Cardiovasc Med* 2008;5:91–102.
16. Fujii K, Kobayashi Y, Mintz GS, et al. Intravascular ultrasound assessment of ulcerated ruptured plaques: a comparison of culprit and nonculprit lesions of patients with acute coronary syndromes and lesions in patients without acute coronary syndromes. *Circulation* 2003;108:2473–8.
17. Wang JC, Normand SL, Mauri L, et al. Coronary artery spatial distribution of acute myocardial infarction occlusions. *Circulation* 2004;110:278–84.
18. Hong MK, Mintz GS, Lee CW, et al. The site of plaque rupture in native coronary arteries: a three-vessel intravascular ultrasound analysis. *J Am Coll Cardiol* 2005;46:261–5.
19. Valgimigli M, Rodriguez-Granillo GA, Garcia-Garcia HM, et al. Distance from the ostium as an independent determinant of coronary plaque composition in vivo: an intravascular ultrasound study based radiofrequency data analysis in humans. *Eur Heart J* 2006;27:655–63.
20. Glaser R, Selzer F, Faxon DP, et al. Clinical progression of incidental, asymptomatic lesions discovered during culprit vessel coronary intervention. *Circulation* 2005;111:143–9.
21. Kaski JC, Chester MR, Chen L, et al. Rapid angiographic progression of coronary artery disease in patients with angina pectoris: the role of complex stenosis morphology. *Circulation* 1995;92:2058–65.
22. Berry C, L'Allier PL, Grégoire J, et al. Comparison of intravascular ultrasound and quantitative coronary angiography for the assessment of coronary artery disease progression. *Circulation* 2007;115:1851–7.
23. Rodriguez-Granillo GA, Serruys PW, McFadden E, et al. First in man prospective evaluation of temporal changes in coronary plaque composition by in vivo intravascular ultrasound radiofrequency data analysis: an integrated biomarker and imaging study (IBIS) substudy. *Eurointervention* 2005;1:282–8.
24. Serruys PW, García-García HM, Buszman P, et al. Effects of the direct lipoprotein-associated phospholipase A<sub>2</sub> inhibitor darapladib on human coronary atherosclerotic plaque. *Circulation* 2008;118:1172–82.

**Key Words:** atherosclerosis ■ coronary disease ■ intravascular ultrasound ■ virtual histology.